


9-16-2010

Two-Loop Soft Anomalous Dimensions for Single Top Quark Associated Production with a W- or H-

Nikolaos Kidonakis

Kennesaw State University, nkidonak@kennesaw.edu

Follow this and additional works at: <https://digitalcommons.kennesaw.edu/facpubs>

 Part of the [Atomic, Molecular and Optical Physics Commons](#), [Elementary Particles and Fields and String Theory Commons](#), and the [Nuclear Commons](#)

Recommended Citation

Kidonakis N. 2010. Two-loop soft anomalous dimensions for single top quark associated production with a W- or H-. *Phys Rev D* 82(5):054018.

This Article is brought to you for free and open access by DigitalCommons@Kennesaw State University. It has been accepted for inclusion in Faculty Publications by an authorized administrator of DigitalCommons@Kennesaw State University. For more information, please contact digitalcommons@kennesaw.edu.

Two-loop soft anomalous dimensions for single top quark associated production with a W^- or H^-

Nikolaos Kidonakis

*Kennesaw State University, Physics #1202,
1000 Chastain Rd., Kennesaw, GA 30144-5591, USA*

Abstract

I present results for the two-loop soft anomalous dimensions for associated production of a single top quark with a W boson or a charged Higgs boson. The calculation uses expressions for the massive cusp anomalous dimension, which are presented in different forms, and it allows soft-gluon resummation at next-to-next-to-leading-logarithm (NNLL) accuracy. From the NNLL resummed cross section I derive approximate NNLO cross sections for $bg \rightarrow tW^-$ and $bg \rightarrow tH^-$ at LHC energies of 7, 10, and 14 TeV.

1 Introduction

The Large Hadron Collider (LHC) will produce top quarks via top-antitop pair or single top quark processes with relatively large cross sections. Given the importance of the top quark [1] to electroweak and Higgs physics, and the observation of single top events at the Tevatron [2, 3, 4], it is crucial to have a good theoretical understanding of top quark production cross sections. An interesting channel to study is associated production of a top quark with a W boson, $bg \rightarrow tW^-$, which is sensitive to new physics and allows a direct measurement of the V_{tb} CKM matrix element. This process is very small at the Tevatron but has the second highest cross section among single top processes at the LHC. A related process is associated production of a top quark with a charged Higgs boson, $bg \rightarrow tH^-$. Charged Higgs bosons appear in the Minimal Supersymmetric Standard Model (MSSM) and other two-Higgs-doublet models (2HDM). In the MSSM there are two Higgs doublets, one giving mass to the up-type fermions and the other to the down-type fermions. Among the extra Higgs particles in the MSSM are two charged Higgs bosons, H^+ and H^- , and the associated production of a top quark with a charged Higgs is a process that the LHC has good potential to observe. Since a central mission of the LHC is to find the Higgs boson and another is to look for supersymmetry, the associated production of a charged Higgs with a top quark is an important channel to study.

The next-to-leading order (NLO) corrections to $bg \rightarrow tW^-$ were calculated in [5] and to $bg \rightarrow tH^-$ in [6, 7, 8]. These processes are very similar with respect to QCD corrections and they have the same color structure. Soft-gluon emission is an important contributor to higher-order corrections, particularly near partonic threshold. The soft-gluon corrections can be formally resummed to all orders in perturbation theory. The resummation follows from the factorization of the cross section into a hard-scattering function H and a soft function S that describes noncollinear soft-gluon emission in the process [9, 10]. The renormalization group evolution of the soft function is controlled by a process-dependent soft anomalous dimension Γ_S . The calculation of Γ_S is performed in the eikonal approximation, which describes the emission of

soft gluons from partons in the hard scattering and leads to modified Feynman rules in diagram calculations. At next-to-leading-logarithm (NLL) accuracy these corrections were resummed for tW^- production at the Tevatron and at the LHC in [10, 11, 12], while the corrections for tH^- production were presented in [13, 14]. These results involved the calculations of the one-loop soft anomalous dimension for these processes.

Recent developments in two-loop calculations [15, 16, 17] have now made possible the resummation of next-to-next-to-leading-logarithm (NNLL) corrections for QCD processes. Here we begin by calculating the two-loop soft (cusp) anomalous dimension for two massive quarks, and then using these results in the limit when one quark is massive (top quark) and one is massless (bottom quark) we calculate the diagrams for associated single top quark production. Since there are three colored partons in the partonic processes $bg \rightarrow tW^-$ and $bg \rightarrow tH^-$ there are many diagrams to consider but the end result for the two-loop soft anomalous dimension for these processes can be written in a simple formula. We then use those results to calculate approximate next-to-next-to-leading order (NNLO) cross sections for tW^- and tH^- production at the LHC.

2 Two-loop soft (cusp) anomalous dimension for a heavy quark-antiquark pair

We begin by presenting the calculation of the two-loop cusp anomalous dimension, which is the soft anomalous dimension for $e^+e^- \rightarrow t\bar{t}$ [15, 16].

We expand the soft (cusp) anomalous dimension as $\Gamma_S = (\alpha_s/\pi)\Gamma_S^{(1)} + (\alpha_s/\pi)^2\Gamma_S^{(2)} + \dots$, The one-loop soft anomalous dimension, $\Gamma_S^{(1)}$, can be read off the coefficient of the ultraviolet (UV) poles of the one-loop diagrams in Fig. 1.

In the eikonal approximation, as the gluon momentum goes to zero, the quark-gluon vertex reduces to $g_s T_F^c v^\mu / v \cdot k$, with g_s the strong coupling, v a dimensionless velocity vector, k the gluon momentum, and T_F^c the generators of SU(3) in the fundamental representation. For example the integral for the diagram in Fig. 1(a) is given by

$$\frac{\alpha_s}{\pi} I_{1a} = g_s^2 \int \frac{d^n k}{(2\pi)^n} \frac{(-i)g_{\mu\nu}}{k^2} \frac{v_i^\mu}{v_i \cdot k} \frac{(-v_j^\nu)}{(-v_j \cdot k)} \quad (2.1)$$

where i labels the quark and j the antiquark. The quark and antiquark velocity vectors obey the relations $v_i \cdot v_j = (1 + \beta^2)/2$ and $v_i^2 = v_j^2 = (1 - \beta^2)/2$, where $\beta = \sqrt{1 - 4m^2/s}$ with m the heavy quark mass and s the center-of-mass energy squared. The eikonal diagrams are calculated in dimensional regularization with $n = 4 - \epsilon$ using Feynman gauge in momentum space.

We find the one-loop soft (cusp) anomalous dimension

$$\Gamma_S^{(1)} = C_F \left[-\frac{(1 + \beta^2)}{2\beta} \ln \left(\frac{1 - \beta}{1 + \beta} \right) - 1 \right] \quad (2.2)$$

where $C_F = (N_c^2 - 1)/(2N_c)$ with $N_c = 3$ the number of colors. This result can also be written in terms of the cusp angle [18] $\gamma = \ln[(1 + \beta)/(1 - \beta)]$, with $\coth \gamma = (1 + \beta^2)/(2\beta)$, as

$$\Gamma_S^{(1)} = C_F(\gamma \coth \gamma - 1). \quad (2.3)$$

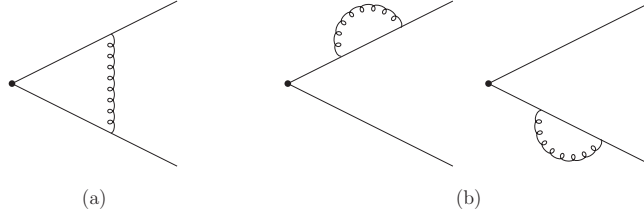


Figure 1: One-loop cusp diagrams with heavy-quark eikonal lines.

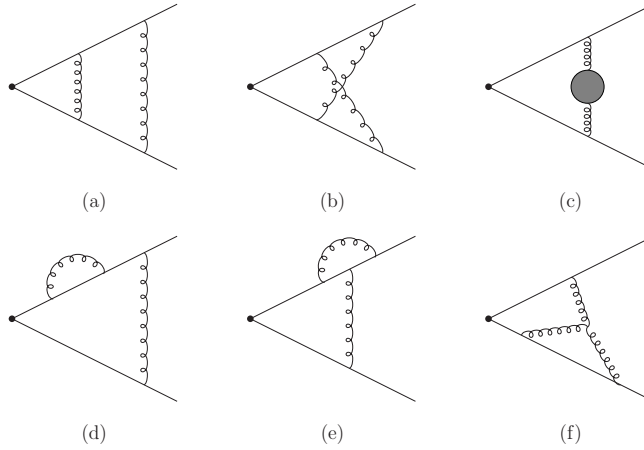


Figure 2: Two-loop cusp vertex diagrams with heavy-quark eikonal lines.

We now continue with the two-loop diagrams. In Fig. 2 we show graphs with vertex corrections and in Fig. 3 graphs with heavy-quark self-energy corrections. The dark blobs in Figs. 2(c) and 3(b) denote quark, gluon, and ghost loops. The black blob in Fig. 3(a) denotes three kinds of corrections shown in Fig. 4. We do not show graphs with gluon loops involving four-gluon vertices and graphs involving three-gluon vertices with all three gluons attaching to a single eikonal line since such graphs have vanishing contributions. For each diagram we include the appropriate one-loop counterterms for the divergent subdiagrams. The calculations are challenging because of the presence of the heavy quark mass. Dimensionally-regularized integrals needed in the calculation are shown in Appendix A. Using the results in Appendix A, the UV poles of the integrals for each diagram are provided in Appendix B.

Combining the kinematic results in Appendix B with color and symmetry factors, the contribution of the diagrams in Figs. 2 and 3 to the two-loop soft (cusp) anomalous dimension is

$$\begin{aligned}
& C_F^2 [I_{2a} + I_{2b} + 2 I_{2d} + 2 I_{2e} + I_{3a1} + I_{3a2} + I_{3c}] \\
+ & C_F C_A \left[-\frac{1}{2} I_{2b} + I_{2f} - I_{2cg} - I_{2e} - I_{3bg} - \frac{1}{2} I_{3a2} \right] + \frac{1}{2} C_F [I_{2cq} + I_{3bq}]
\end{aligned}$$

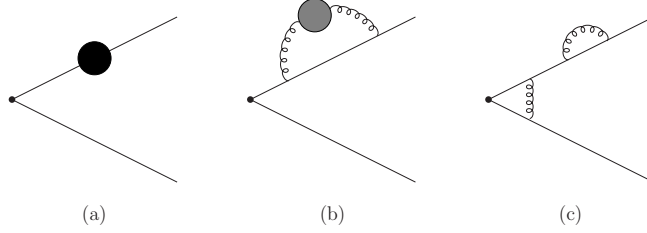


Figure 3: Two-loop cusp self-energy diagrams with heavy-quark eikonal lines.

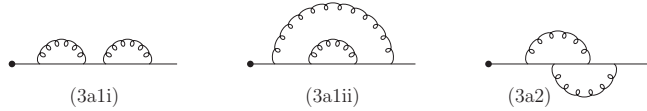


Figure 4: Detail of the black blob of Fig. 3(a).

$$= -\frac{1}{2\epsilon^2} \left(\Gamma_S^{(1)} \right)^2 + \frac{\beta_0}{4\epsilon^2} \Gamma_S^{(1)} - \frac{1}{2\epsilon} \Gamma_S^{(2)} \quad (2.4)$$

where I_k denotes the integral for diagram k , e.g. I_{2d} is the integral for diagram 2(d). Also I_{2cq} and I_{3bq} denote the quark-loop contribution in Figs. 2(c) and 3(b), respectively, while I_{2cg} and I_{3bg} denote the gluon-loop plus ghost-loop contributions to the respective diagrams. I_{3a1} denotes the sum of the graphs 3(a1i) and 3(a1ii) detailed in Fig. 4 while I_{3a2} is the integral for the last graph in Fig. 4. On the right-hand side of Eq. (2.4) in addition to the two-loop soft anomalous dimension, $\Gamma_S^{(2)}$, which appears in the coefficient of the $1/\epsilon$ pole, there also appear terms from the exponentiation of the one-loop result and the running of the coupling which account for all the double poles of the graphs. Here $\beta_0 = (11/3)C_A - 2n_f/3$, with $C_A = N_c$ and n_f the number of light quark flavors. From Eq. (2.4) we solve for the two-loop soft (cusp) anomalous dimension:

$$\Gamma_S^{(2)} = \frac{K}{2} \Gamma_S^{(1)} + C_F C_A M_\beta \quad (2.5)$$

where

$$\begin{aligned} M_\beta &= \frac{1}{2} + \frac{\zeta_2}{2} + \frac{1}{2} \ln^2 \left(\frac{1-\beta}{1+\beta} \right) \\ &- \frac{(1+\beta^2)^2}{8\beta^2} \left[\zeta_3 + \zeta_2 \ln \left(\frac{1-\beta}{1+\beta} \right) + \frac{1}{3} \ln^3 \left(\frac{1-\beta}{1+\beta} \right) + \ln \left(\frac{1-\beta}{1+\beta} \right) \text{Li}_2 \left(\frac{(1-\beta)^2}{(1+\beta)^2} \right) - \text{Li}_3 \left(\frac{(1-\beta)^2}{(1+\beta)^2} \right) \right] \\ &- \frac{(1+\beta^2)}{4\beta} \left[\zeta_2 - \zeta_2 \ln \left(\frac{1-\beta}{1+\beta} \right) + \ln^2 \left(\frac{1-\beta}{1+\beta} \right) - \frac{1}{3} \ln^3 \left(\frac{1-\beta}{1+\beta} \right) + 2 \ln \left(\frac{1-\beta}{1+\beta} \right) \ln \left(\frac{(1+\beta)^2}{4\beta} \right) \right. \\ &\quad \left. - \text{Li}_2 \left(\frac{(1-\beta)^2}{(1+\beta)^2} \right) \right]. \end{aligned} \quad (2.6)$$

We have written the two-loop result $\Gamma_S^{(2)}$ in Eq. (2.5) in the form of a term which is a multiple of the one-loop soft anomalous dimension $\Gamma_S^{(1)}$, Eq. (2.2), plus a set of additional terms which

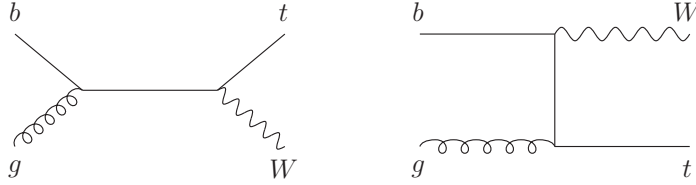


Figure 5: Leading-order diagrams for $bg \rightarrow tW^-$.

have been denoted as M_β . Here $\zeta_2 = \pi^2/6$ and $\zeta_3 = 1.2020569\dots$. The well-known two-loop constant K [19] is given by $K = C_A(67/18 - \zeta_2) - 5n_f/9$. The color structure of $\Gamma_S^{(2)}$ involves only the factors $C_F C_A$ and $C_F n_f$. Note that as $\beta \rightarrow 1$, $M_\beta \rightarrow (1 - \zeta_3)/2$.

The result in Eq. (2.5) can be written in terms of the cusp angle γ as

$$\Gamma_S^{(2)} = \frac{K}{2} \Gamma_S^{(1)} + C_F C_A \left\{ \frac{1}{2} + \frac{\zeta_2}{2} + \frac{\gamma^2}{2} - \frac{1}{2} \coth^2 \gamma \left[\zeta_3 - \zeta_2 \gamma - \frac{\gamma^3}{3} - \gamma \text{Li}_2(e^{-2\gamma}) - \text{Li}_3(e^{-2\gamma}) \right] - \frac{1}{2} \coth \gamma \left[\zeta_2 + \zeta_2 \gamma + \gamma^2 + \frac{\gamma^3}{3} + 2\gamma \ln(1 - e^{-2\gamma}) - \text{Li}_2(e^{-2\gamma}) \right] \right\}, \quad (2.7)$$

and is in agreement, but in a simpler and more explicit form, with the result for the cusp anomalous dimension of Ref. [18].

3 Two-loop soft anomalous dimension and NNLL resummation for $bg \rightarrow tW^-$ and $bg \rightarrow tH^-$

We now turn our attention to processes that involve a bottom quark, a gluon, and a top quark as the colored particles in the hard scattering, namely tW^- and tH^- production. The leading-order diagrams for $bg \rightarrow tW^-$ are shown in Fig. 5; if one replaces the W^- by an H^- the graphs describe $bg \rightarrow tH^-$. We treat the bottom quark as massless [13]. In this section we calculate the two-loop soft anomalous dimension that will allow us to resum the soft-gluon contributions to NNLL accuracy.

In Fig. 6 we show the one-loop eikonal diagrams for these processes. Calculating the integrals associated with these diagrams we find the one-loop soft anomalous dimension for $bg \rightarrow tW^-$:

$$\Gamma_{S,tW^-}^{(1)} = C_F \left[\ln \left(\frac{m_t^2 - t}{m_t \sqrt{s}} \right) - \frac{1}{2} \right] + \frac{C_A}{2} \ln \left(\frac{m_t^2 - u}{m_t^2 - t} \right) \quad (3.1)$$

where $s = (p_b + p_g)^2$, $t = (p_b - p_t)^2$, $u = (p_g - p_t)^2$, and m_t is the top quark mass. The expression for $bg \rightarrow tH^-$ is identical. This result is slightly different from the result in Ref. [10, 13] because the axial gauge was used in those papers, while the result in Eq. (3.1) is calculated in Feynman gauge. Of course these differences are compensated by other terms in the resummed formula and the final result for the cross section is independent of the choice of gauge.

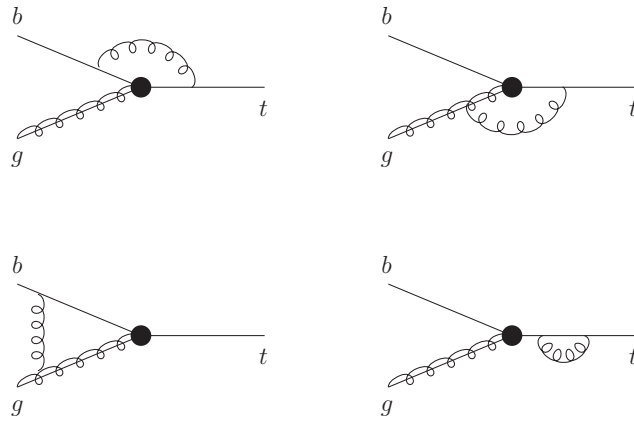


Figure 6: One-loop eikonal diagrams with bottom quark-gluon-top quark vertex.

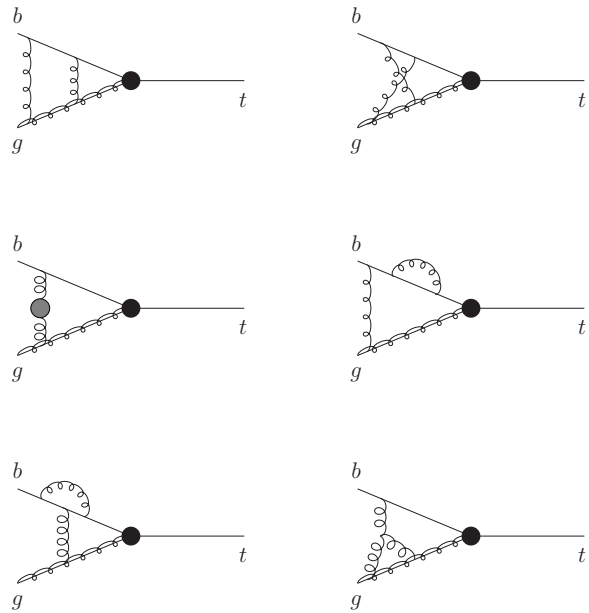


Figure 7: Two-loop eikonal diagrams involving the bottom quark and gluon eikonal lines.

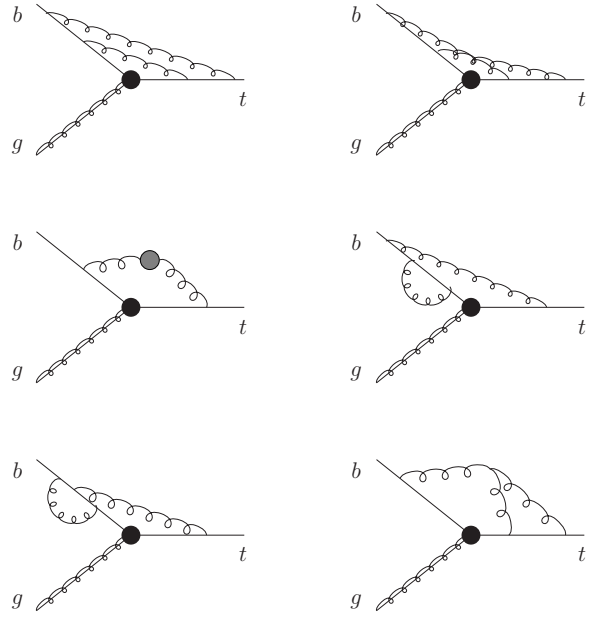


Figure 8: Two-loop eikonal diagrams involving the bottom quark and top quark eikonal lines.

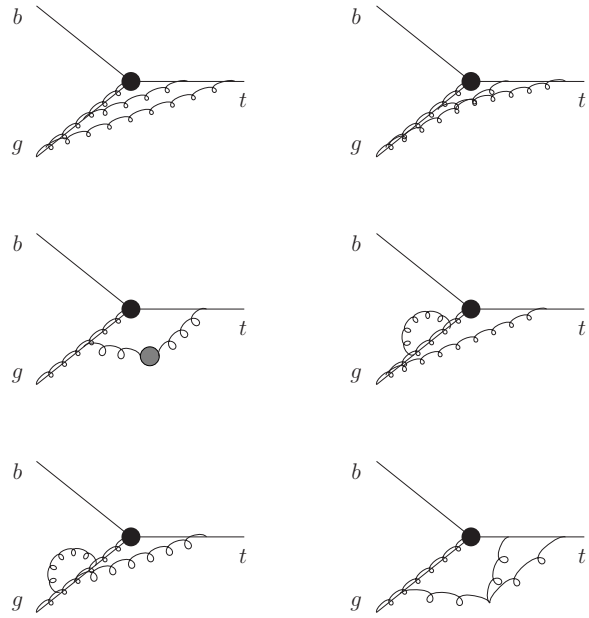


Figure 9: Two-loop eikonal diagrams involving the gluon and top quark eikonal lines.

To find the two-loop soft anomalous dimension we calculate the diagrams shown in Figs. 7, 8, 9, plus diagrams involving the top-quark self energy as in Figs. 3 and 4. Since they are three colored partons, with one of them massive, we calculate diagrams that contribute to the cusp anomalous dimension for each pair of partons using the results in the previous section in the limit when one or both partons are massless. Note that diagrams that involve gluons attached to all three eikonal lines either vanish or do not contribute to the two-loop result [20], and hence we do not show them. Combining the kinematic results for the integrals from Appendix B with color and symmetry factors we have

$$\begin{aligned}
& \frac{C_A^2}{4} [I_{2a} + 2 I_{2b} + 2 I_{2cg} + 2 I_{2e} - 2 I_{2f}]_{bt} + C_F^2 [I_{2a} + I_{2b} + 2 I_{2d} + 2 I_{2e} + I_{3a} + I_{3c}]_{bt} \\
& + C_F C_A \left[-I_{2a} - \frac{3}{2} I_{2b} - I_{2cg} - I_{2d} - 2 I_{2e} + I_{2f} - I_{3bg} - \frac{1}{2} I_{3a2} - \frac{1}{2} I_{3c} \right]_{bt} - \frac{C_A}{4} [I_{2cq}]_{bt} \\
& + \frac{1}{2} C_F [I_{2cq} + I_{3bq}]_{bt} + \frac{C_A^2}{4} [I_{2a} - 2 I_{2cg} + 2 I_{2d} + 2 I_{2f}]_{bg} + \frac{C_A}{4} [I_{2cq}]_{bg} \\
& + \frac{C_A^2}{4} [I_{2a} - 2 I_{2cg} + 2 I_{2d} + 2 I_{2f}]_{gt} + \frac{C_A}{4} [I_{2cq}]_{gt} + C_F C_A \frac{1}{2} [I_{3c}]_{gt} + I_{3\text{-line}} \\
& = -\frac{1}{2\epsilon^2} \left(\Gamma_{S,tW^-}^{(1)} \right)^2 + \frac{\beta_0}{4\epsilon^2} \Gamma_{S,tW^-}^{(1)} - \frac{1}{2\epsilon} \Gamma_{S,tW^-}^{(2)} \tag{3.2}
\end{aligned}$$

where $I_{3\text{-line}}$ denotes the terms involving gluons attached to all three lines that do not contribute at two loops and $[I_{2d}]_{bt}$, for example, stands for the 2(d)-type diagram in Fig. 8 involving the b and t quarks.

We thus find the two-loop soft-anomalous dimension for $bg \rightarrow tW^-$

$$\Gamma_{S,tW^-}^{(2)} = \frac{K}{2} \Gamma_{S,tW^-}^{(1)} + C_F C_A \frac{(1 - \zeta_3)}{4} \tag{3.3}$$

where $\Gamma_{S,tW^-}^{(1)}$ is given in Eq. (3.1). The result for $bg \rightarrow tH^-$ is the same.

With the two-loop soft-anomalous dimension at hand we are now ready to resum the soft-gluon corrections at NNLL accuracy. For tW^- production the resummed partonic cross section in moment space (with N the moment variable) is given by [9, 10, 17, 21]

$$\begin{aligned}
\hat{\sigma}^{res}(N) &= \exp [E_q(N_q) + E_g(N_g)] \exp \left[2 \int_{\mu_F}^{\sqrt{s}} \frac{d\mu}{\mu} \left(\gamma_{q/q}(\tilde{N}_q, \alpha_s(\mu)) + \gamma_{g/g}(\tilde{N}_g, \alpha_s(\mu)) \right) \right] \\
&\times H^{bg \rightarrow tW^-}(\alpha_s(\sqrt{s})) S^{bg \rightarrow tW^-}(\alpha_s(\sqrt{s}/\tilde{N}')) \exp \left[2 \int_{\sqrt{s}}^{\sqrt{s}/\tilde{N}'} \frac{d\mu}{\mu} \Gamma_{S,tW^-}(\alpha_s(\mu)) \right] \tag{3.4}
\end{aligned}$$

and similarly for tH^- production.

The first exponent [22, 23] in the above expression resums soft and collinear corrections from the incoming partons

$$E_i(N_i) = \int_0^1 dz \frac{z^{N_i-1} - 1}{1-z} \left\{ \int_1^{(1-z)^2} \frac{d\lambda}{\lambda} A_i(\alpha_s(\lambda s)) + D_i[\alpha_s((1-z)^2 s)] \right\} \tag{3.5}$$

where i stands for the incoming bottom quark ($i = q$) or the incoming gluon ($i = g$). Here $N_q = N[(m_W^2 - u)/m_t^2]$ and $N_g = N[(m_W^2 - t)/m_t^2]$ where m_W is the W -boson mass. The quantity

A_i has a perturbative expansion, $A_i = \sum_n (\alpha_s/\pi)^n A_i^{(n)}$. Here $A_q^{(1)} = C_F$ and $A_q^{(2)} = C_F K/2$, while $A_g^{(1)} = C_A$ and $A_g^{(2)} = C_A K/2$.

Also $D_i = \sum_n (\alpha_s/\pi)^n D_i^{(n)}$, with $D_q^{(1)} = D_g^{(1)} = 0$, and [24]

$$D_q^{(2)} = C_F C_A \left(-\frac{101}{54} + \frac{11}{6} \zeta_2 + \frac{7}{4} \zeta_3 \right) + C_F n_f \left(\frac{7}{27} - \frac{\zeta_2}{3} \right) \quad (3.6)$$

and $D_g^{(2)} = (C_A/C_F) D_q^{(2)}$.

In the third exponent $\gamma_{i/i}$ is the moment-space anomalous dimension of the $\overline{\text{MS}}$ parton density $\phi_{i/i}$ and it controls the factorization scale, μ_F , dependence of the cross section. We have $\gamma_{i/i} = -A_i \ln \tilde{N}_i + \gamma_i$ where A_i was defined above, $\tilde{N}_i = N_i e^{\gamma_E}$ with γ_E the Euler constant, and the parton anomalous dimension $\gamma_i = \sum_n (\alpha_s/\pi)^n \gamma_i^{(n)}$ where $\gamma_q^{(1)} = 3C_F/4$ and $\gamma_g^{(1)} = \beta_0/4$.

$H^{bg \rightarrow tW}$ is the hard-scattering function while $S^{bg \rightarrow tW}$ is the soft function describing non-collinear soft gluon emission [9, 10]. The evolution of the soft function is controlled by the soft anomalous dimension Γ_{S,tW^-} . Here $\tilde{N}' = \tilde{N}(s/m_t^2)$ with $\tilde{N} = N e^{\gamma_E}$.

For tH^- production the resummed formula is essentially the same. The only difference, apart from the obvious use of the appropriate hard-scattering function for this process, is the definition of N_q and N_g . In this case, $N_q = N[(m_{H^-}^2 - u)/m_{H^-}^2]$ and $N_g = N[(m_{H^-}^2 - t)/m_{H^-}^2]$ where m_{H^-} is the charged Higgs mass.

The resummed cross section, Eq. (3.4), can be expanded in the strong coupling, α_s , and inverted to momentum space, thus providing fixed-order results for the soft-gluon corrections. The NLO expansion of the resummed cross section after inversion to momentum space is

$$\hat{\sigma}^{(1)} = \sigma^B \frac{\alpha_s(\mu_R)}{\pi} \{ c_3 \mathcal{D}_1(s_4) + c_2 \mathcal{D}_0(s_4) \}, \quad (3.7)$$

where σ^B is the Born term for the process and μ_R is the renormalization scale. We use the notation $\mathcal{D}_k(s_4) = [\ln^k(s_4/m_t^2)/s_4]_+$ in tW^- production and $\mathcal{D}_k(s_4) = [\ln^k(s_4/m_{H^-}^2)/s_4]_+$ in tH^- production for the plus distributions involving logarithms of a kinematical variable s_4 that measures distance from threshold ($s_4 = 0$ at threshold). For $bg \rightarrow tW^-$, $s_4 = s+t+u-m_t^2-m_W^2$, while for $bg \rightarrow tH^-$, $s_4 = s+t+u-m_t^2-m_{H^-}^2$. The coefficient of the leading term is

$$c_3 = 2(A_q^{(1)} + A_g^{(1)}). \quad (3.8)$$

The coefficient of the next-to-leading term, c_2 , can be written as $c_2 = c_2^\mu + T_2$, with c_2^μ denoting the terms involving logarithms of the scale and T_2 denoting the scale-independent terms. For $bg \rightarrow tW^-$

$$c_2^\mu = -(A_q^{(1)} + A_g^{(1)}) \ln \left(\frac{\mu_F^2}{m_t^2} \right) \quad (3.9)$$

and

$$T_2 = -2 A_q^{(1)} \ln \left(\frac{m_W^2 - u}{m_t^2} \right) - 2 A_g^{(1)} \ln \left(\frac{m_W^2 - t}{m_t^2} \right) - (A_q^{(1)} + A_g^{(1)}) \ln \left(\frac{m_t^2}{s} \right) + 2 \Gamma_{S,tW^-}^{(1)}. \quad (3.10)$$

For $bg \rightarrow tH^-$ replace both m_W and m_t in the above two equations by m_{H^-} .

As discussed in [10, 13] the expansion can also determine the terms involving logarithms of the factorization and renormalization scales in the coefficient, c_1 , of the $\delta(s_4)$ terms. If we denote these terms as c_1^μ , then for tW^- production

$$c_1^\mu = \left[A_q^{(1)} \ln \left(\frac{m_W^2 - u}{m_t^2} \right) + A_g^{(1)} \ln \left(\frac{m_W^2 - t}{m_t^2} \right) - \gamma_q^{(1)} - \gamma_g^{(1)} \right] \ln \left(\frac{\mu_F^2}{m_t^2} \right) + \frac{\beta_0}{4} \ln \left(\frac{\mu_R^2}{m_t^2} \right), \quad (3.11)$$

while for $bg \rightarrow tH^-$ replace both m_W and m_t in the above equation by m_{H^-} . The full virtual terms are not derivable from resummation, which addresses soft-gluon contributions, but can be taken from the complete NLO calculation.

The NNLO expansion of the resummed cross section for $bg \rightarrow tW^-$ after inversion to momentum space is

$$\begin{aligned} \hat{\sigma}^{(2)} = & \sigma^B \frac{\alpha_s^2(\mu_R)}{\pi^2} \left\{ \frac{1}{2} c_3^2 \mathcal{D}_3(s_4) + \left[\frac{3}{2} c_3 c_2 - \frac{\beta_0}{4} c_3 \right] \mathcal{D}_2(s_4) \right. \\ & + \left[c_3 c_1 + c_2^2 - \zeta_2 c_3^2 - \frac{\beta_0}{2} T_2 + \frac{\beta_0}{4} c_3 \ln \left(\frac{\mu_R^2}{m_t^2} \right) + 2A_q^{(2)} + 2A_g^{(2)} \right] \mathcal{D}_1(s_4) \\ & + \left[c_2 c_1 - \zeta_2 c_3 c_2 + \zeta_3 c_3^2 + \frac{\beta_0}{4} c_2 \ln \left(\frac{\mu_R^2}{s} \right) - \frac{\beta_0}{2} A_q^{(1)} \ln^2 \left(\frac{m_W^2 - u}{m_t^2} \right) - \frac{\beta_0}{2} A_g^{(1)} \ln^2 \left(\frac{m_W^2 - t}{m_t^2} \right) \right. \\ & \quad - 2A_q^{(2)} \ln \left(\frac{m_W^2 - u}{m_t^2} \right) - 2A_g^{(2)} \ln \left(\frac{m_W^2 - t}{m_t^2} \right) + D_q^{(2)} + D_g^{(2)} \\ & \quad \left. + \frac{\beta_0}{8} (A_q^{(1)} + A_g^{(1)}) \ln^2 \left(\frac{\mu_F^2}{s} \right) - (A_q^{(2)} + A_g^{(2)}) \ln \left(\frac{\mu_F^2}{s} \right) + 2\Gamma_{S,tW^-}^{(2)} \right] \mathcal{D}_0(s_4) \left. \right\}. \quad (3.12) \end{aligned}$$

For $bg \rightarrow tH^-$ again replace both m_W and m_t by m_{H^-} in the above equation. It is important to note that all NNLO soft-gluon corrections are derived from the NNLL resummed cross section, i.e. the coefficients of all powers of logarithms in s_4 are given in Eq. (3.12), from $\mathcal{D}_3(s_4)$ down to $\mathcal{D}_0(s_4)$. In Ref. [10] and [13, 14], where NLL accuracy was attained, only the coefficients of $\mathcal{D}_3(s_4)$ and $\mathcal{D}_2(s_4)$ were fully determined. Thus, at NNLL accuracy the theoretical improvement over NLL is significant. As discussed in [10, 14] additional $\delta(s_4)$ terms involving the factorization and renormalization scales are also computed.

4 NNLO approximate cross sections for tW^- and tH^- production at the LHC

We now use the results of the previous section to calculate approximate NNLO cross sections for $bg \rightarrow tW^-$ and $bg \rightarrow tH^-$ at the LHC.

We begin with tW^- production. As has been shown in [10, 11] the NLO expansion of the resummed cross section approximates well the complete NLO result for both Tevatron and LHC energies. In fact when damping factors are used to limit the soft-gluon contributions far away from threshold, as was also used for $t\bar{t}$ production [25] and s -channel single-top production [17], then the approximation is excellent. This shows that soft-gluon corrections are dominant for this process.

NNLO approx (NNLL) tW^- cross section (pb)			
m_t (GeV)	LHC 7 TeV	LHC 10 TeV	LHC 14 TeV
170	8.24	20.3	43.6
171	8.09	20.0	43.0
172	7.94	19.7	42.4
173	7.80	19.4	41.8
174	7.66	19.1	41.2
175	7.53	18.7	40.6

Table 1: The $bg \rightarrow tW^-$ production cross section in pb in pp collisions at the LHC with $\sqrt{S} = 7$ TeV, 10 TeV, and 14 TeV, with $\mu = m_t$ and using the MSTW2008 NNLO pdf [26]. The approximate NNLO results are shown at NNLL accuracy.

In Table 1 we provide numerical values for the tW^- cross section at the LHC for energies of 7, 10, and 14 TeV and a range of top quark masses from 170 to 175 GeV. The NNLO approximate corrections increase the NLO cross section by $\sim 8\%$. We note that the cross section for $\bar{b}g \rightarrow \bar{t}W^+$ is identical.

At 7 TeV with $m_t = 173$ GeV the approximate NNLO cross section from NNLL resummation is

$$\sigma_{tW^-}^{\text{NNLOapprox}}(m_t = 173 \text{ GeV}, 7 \text{ TeV}) = 7.8 \pm 0.2_{-0.6}^{+0.5} \text{ pb}. \quad (4.1)$$

The first uncertainty is from scale variation between $m_t/2$ and $2m_t$ and the second is from the MSTW2008 NNLO pdf at 90% C.L. At 10 TeV, again with $m_t = 173$ GeV, the cross section is $19.4 \pm 0.5_{-1.1}^{+1.0}$ pb, and at 14 TeV we find $41.8 \pm 1.0_{-2.4}^{+1.5}$ pb.

In Fig. 10 we plot the $bg \rightarrow tW^-$ NNLO approximate cross section from NNLL resummation at the LHC versus top quark mass for energies of 7, 10, and 14 TeV.

Next we consider the process $bg \rightarrow tH^-$. The ratio of the vacuum expectation values, v_2, v_1 for the two Higgs doublets is $\tan \beta = v_2/v_1$, and the value of the cross section depends on the choice of this undetermined parameter. However, the overall percentage enhancement of the cross section from the higher-order soft-gluon corrections is independent of the value of $\tan \beta$.

In Fig. 11 we plot the $bg \rightarrow tH^-$ NNLO approximate cross section from NNLL resummation at the LHC versus charged Higgs mass for energies of 7, 10, and 14 TeV, using a value of $\tan \beta = 30$. The NNLO approximate corrections increase the NLO cross section by $\sim 15\%$ to $\sim 20\%$ for the range of charged Higgs masses shown. We note that the cross section for $\bar{b}g \rightarrow \bar{t}H^+$ is identical (assuming the underlying model is CP conserving).

5 Conclusion

The cross sections for associated production of a single top quark with a W boson or with a charged Higgs boson receive large contributions from soft gluon corrections. These contributions were resummed in this paper to NNLL accuracy, thus extending previous NLL results. Attaining this accuracy requires the calculation of two-loop soft anomalous dimensions from the UV poles of dimensionally regularized integrals of two-loop eikonal diagrams. First the two-loop cusp

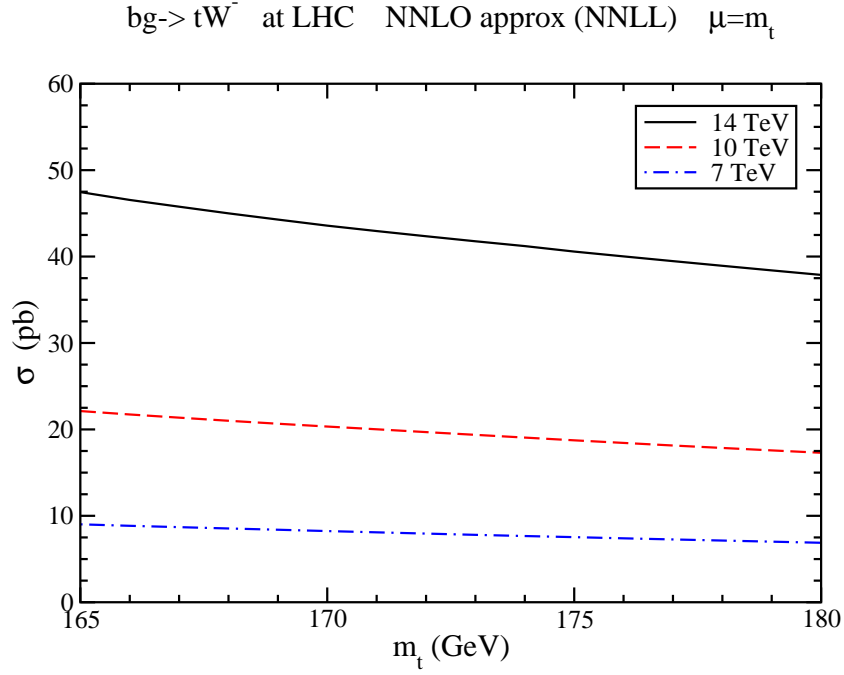


Figure 10: The cross section for tW^- production at the LHC with $\sqrt{S} = 7$ TeV, 10 TeV, and 14 TeV, and MSTW2008 NNLO pdf.

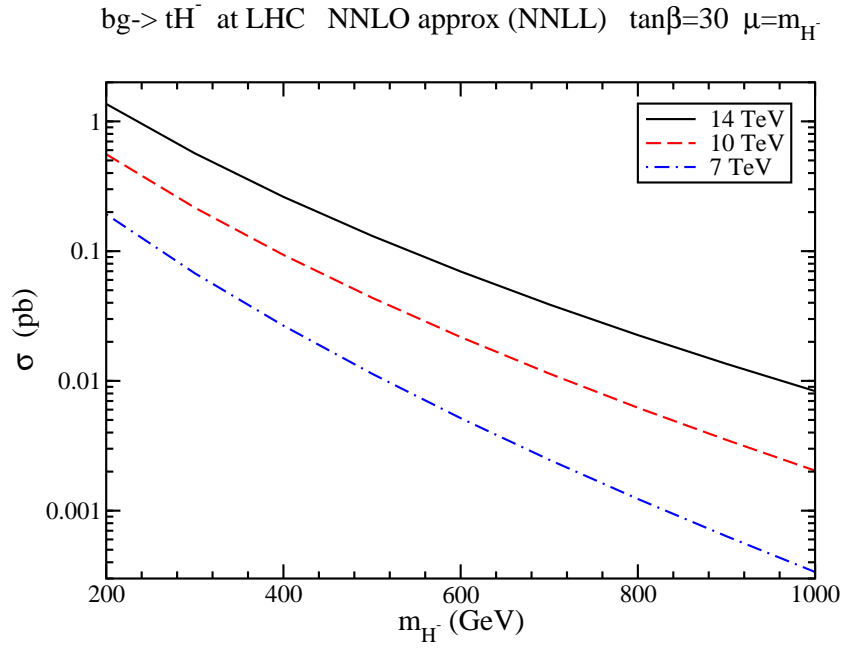


Figure 11: The cross section for tH^- production at the LHC with $\sqrt{S} = 7$ TeV, 10 TeV, and 14 TeV, and MSTW2008 NNLO pdf.

anomalous dimension was calculated, which is an essential ingredient to all NNLL resummations for QCD processes, and then the result was used to calculate the two-loop soft anomalous dimensions for $bg \rightarrow tW^-$ and $bg \rightarrow tH^-$. From the NNLL resummed formula approximate NNLO cross sections were derived and numerical predictions made for tW^- and tH^- production at LHC energies. These approximate NNLO corrections enhance the NLO cross section for tW^- production by $\sim 8\%$ and for tH^- production by $\sim 15\%$ to $\sim 20\%$.

Acknowledgements

This work was supported by the National Science Foundation under Grant No. PHY 0855421.

Appendix A: Dimensionally regularized eikonal integrals

We list results for several dimensionally regularized integrals needed in the calculation of the two-loop soft anomalous dimension.

$$\int \frac{d^n k}{k^2 v_i \cdot k v_j \cdot k} = \frac{i}{\epsilon} (-1)^{-1-\frac{\epsilon}{2}} \pi^{2-\frac{\epsilon}{2}} 2^{3+3\frac{\epsilon}{2}} \Gamma\left(1 + \frac{\epsilon}{2}\right) {}_2F_1\left(\frac{1}{2}, 1 + \frac{\epsilon}{2}; \frac{3}{2}; \beta^2\right) \quad (\text{A.1})$$

where ${}_2F_1$ is the Gauss hypergeometric function.

$$\int \frac{d^n k}{k^2 (v_i \cdot k)^2} = \frac{i}{\epsilon} (-1)^{1-\frac{\epsilon}{2}} \pi^{2-\frac{\epsilon}{2}} 2^{3+3\frac{\epsilon}{2}} (1 - \beta^2)^{-1-\frac{\epsilon}{2}} \Gamma\left(1 + \frac{\epsilon}{2}\right) \quad (\text{A.2})$$

$$\begin{aligned} \int \frac{d^n k}{(k^2)^{1+\frac{\epsilon}{2}} v_i \cdot k v_j \cdot k} &= \frac{i}{\epsilon^2} \frac{(-1)^{1-\epsilon}}{\beta} 2^{2\epsilon} \pi^{2-\frac{\epsilon}{2}} \Gamma(1 + \epsilon) \frac{1}{\Gamma\left(1 + \frac{\epsilon}{2}\right)} \\ &\times \left[(1 - \beta)^{-\epsilon} {}_2F_1\left(-\epsilon, 1 + \epsilon; 1 - \epsilon; \frac{1 - \beta}{2}\right) - (1 + \beta)^{-\epsilon} {}_2F_1\left(-\epsilon, 1 + \epsilon; 1 - \epsilon; \frac{1 + \beta}{2}\right) \right] \end{aligned} \quad (\text{A.3})$$

$$\begin{aligned} \int \frac{d^n k}{k^2 (v_i \cdot k)^{1+\epsilon} v_j \cdot k} &= \frac{i \pi^{2-\frac{\epsilon}{2}}}{\epsilon(1 + \epsilon)} 2^{2+\frac{9\epsilon}{2}} (-1)^{-1-\frac{3\epsilon}{2}} (1 - \beta^2)^{-1-\frac{3\epsilon}{2}} \Gamma\left(1 + \frac{3\epsilon}{2}\right) \frac{1}{\Gamma(1 + \epsilon)} \\ &\times F_1\left[1 + \epsilon; 1 + \frac{3\epsilon}{2}, 1 + \frac{3\epsilon}{2}; 2 + \epsilon; \frac{2\beta}{1 + \beta}, \frac{-2\beta}{1 - \beta}\right] \end{aligned} \quad (\text{A.4})$$

where F_1 is the Appell hypergeometric function.

$$\begin{aligned} \int \frac{d^n k_2}{k_2^2 [v_i \cdot (k_1 + k_2)]^2} &= \frac{i}{\epsilon} \frac{(-1)^{-1+\frac{\epsilon}{2}}}{(1 + \epsilon)} 2^{4-\frac{\epsilon}{2}} \pi^{\frac{3-\epsilon}{2}} (1 - \beta^2)^{-1+\frac{\epsilon}{2}} (v_i \cdot k_1)^{-\epsilon} \\ &\times \Gamma\left(1 + \frac{\epsilon}{2}\right) \Gamma\left(1 - \frac{\epsilon}{2}\right) \Gamma\left(\frac{3 + \epsilon}{2}\right) \end{aligned} \quad (\text{A.5})$$

$$\int \frac{d^n k}{k^2 (v_i \cdot k)^{2+\epsilon}} = \frac{i\pi^{2-\frac{\epsilon}{2}}}{\epsilon(1+\epsilon)} 2^{2+\frac{9\epsilon}{2}} (-1)^{-1-\frac{3\epsilon}{2}} (1-\beta^2)^{-1-\frac{3\epsilon}{2}} \Gamma\left(1+\frac{3\epsilon}{2}\right) \frac{1}{\Gamma(1+\epsilon)} \quad (\text{A.6})$$

$$\begin{aligned} \int \frac{d^n k_1}{k_1^2 v_i \cdot k_1 v_i \cdot (k_1 + k_2)} &= \frac{i}{\epsilon} (-1)^{\frac{\epsilon}{2}} 2^{2-\frac{\epsilon}{2}} \pi^{\frac{3-\epsilon}{2}} (v_i \cdot k_2)^{-\epsilon} (1-\beta^2)^{-1+\frac{\epsilon}{2}} \\ &\times \Gamma\left(1+\frac{\epsilon}{2}\right) \Gamma\left(1-\frac{\epsilon}{2}\right) \Gamma\left(\frac{\epsilon-1}{2}\right) \end{aligned} \quad (\text{A.7})$$

$$\begin{aligned} \int \frac{d^n k_2}{k_2^2 v_i \cdot k_2 [v_i \cdot (k_1 + k_2)]^2} &= \frac{i}{1-\epsilon} (-1)^{1+\frac{\epsilon}{2}} 2^{3-\frac{3\epsilon}{2}} \pi^{2-\frac{\epsilon}{2}} (v_i \cdot k_1)^{-1-\epsilon} \\ &\times (1-\beta^2)^{-1+\frac{\epsilon}{2}} \Gamma\left(1-\frac{\epsilon}{2}\right) \Gamma(1+\epsilon) \end{aligned} \quad (\text{A.8})$$

$$\int \frac{d^n k}{(k^2)^{1+\frac{\epsilon}{2}} (v_i \cdot k)^2} = \frac{i}{\epsilon} (-1)^{-1-\epsilon} 2^{2+3\epsilon} \pi^{2-\frac{\epsilon}{2}} (1-\beta^2)^{-1-\epsilon} \Gamma(1+\epsilon) \frac{1}{\Gamma\left(1+\frac{\epsilon}{2}\right)} \quad (\text{A.9})$$

Appendix B: UV poles of the integrals for eikonal one-loop and two-loop diagrams for the soft (cusp) anomalous dimension

Here we present the UV poles of the integrals for the one-loop eikonal diagrams in Fig. 1 and the two-loop eikonal diagrams in Figs. 2 and 3.

First we list the integrals for the one-loop diagrams

$$I_{1a} = \frac{(1+\beta^2)}{2\beta} \frac{1}{\epsilon} \ln\left(\frac{1-\beta}{1+\beta}\right) \quad (\text{B.1})$$

and

$$I_{1b} = \frac{1}{\epsilon} \quad (\text{B.2})$$

Then we list the integrals for the two-loop diagrams:

$$I_{2a} + I_{2b} = \frac{(1+\beta^2)^2}{8\beta^2} \frac{(-1)}{\epsilon^2} \ln^2\left(\frac{1-\beta}{1+\beta}\right). \quad (\text{B.3})$$

$$I_{2b} = \frac{(1+\beta^2)^2}{8\beta^2} \frac{1}{\epsilon} \left\{ -\frac{1}{3} \ln^3\left(\frac{1-\beta}{1+\beta}\right) - \ln\left(\frac{1-\beta}{1+\beta}\right) \left[\text{Li}_2\left(\frac{(1-\beta)^2}{(1+\beta)^2}\right) + \zeta_2 \right] + \text{Li}_3\left(\frac{(1-\beta)^2}{(1+\beta)^2}\right) - \zeta_3 \right\} \quad (\text{B.4})$$

$$I_{2cq} = n_f \frac{(1+\beta^2)}{6\beta} \left[\frac{1}{\epsilon^2} - \frac{5}{6\epsilon} \right] \ln \left(\frac{1-\beta}{1+\beta} \right) \quad (\text{B.5})$$

$$I_{2cg} = \frac{5}{24} \frac{(1+\beta^2)}{\beta} \left[\frac{1}{\epsilon^2} - \frac{31}{30\epsilon} \right] \ln \left(\frac{1-\beta}{1+\beta} \right) \quad (\text{B.6})$$

$$I_{2d} = \frac{(1+\beta^2)}{4\beta} \left\{ -\frac{1}{\epsilon^2} \ln \left(\frac{1-\beta}{1+\beta} \right) + \frac{1}{\epsilon} \left[\ln \left(\frac{1-\beta}{1+\beta} \right) + \frac{1}{2} \ln^2 \left(\frac{1-\beta}{1+\beta} \right) \right. \right. \\ \left. \left. + \ln \left(\frac{1-\beta}{1+\beta} \right) \ln \left(\frac{(1+\beta)^2}{4\beta} \right) - \frac{1}{2} \text{Li}_2 \left(\frac{(1-\beta)^2}{(1+\beta)^2} \right) + \frac{\zeta_2}{2} \right] \right\} \quad (\text{B.7})$$

$$I_{2e} = -I_{2d} \quad (\text{B.8})$$

$$I_{2f} = \frac{1}{\epsilon} \left\{ -\frac{1}{4} \left[2\zeta_2 + \ln^2 \left(\frac{1-\beta}{1+\beta} \right) \right] \left[\frac{(1+\beta^2)}{2\beta} \ln \left(\frac{1-\beta}{1+\beta} \right) + 1 \right] + \frac{(1+\beta^2)}{12\beta} \ln^3 \left(\frac{1-\beta}{1+\beta} \right) \right\} \quad (\text{B.9})$$

$$I_{3a1} = -\frac{3}{2\epsilon^2} + \frac{1}{2\epsilon}, \quad (\text{B.10})$$

$$I_{3a2} = \frac{1}{\epsilon^2} - \frac{1}{2\epsilon} \quad (\text{B.11})$$

$$I_{3bq} = \frac{n_f}{3} \left[\frac{1}{\epsilon^2} - \frac{5}{6\epsilon} \right] \quad (\text{B.12})$$

$$I_{3bg} = \frac{5}{12} \left[\frac{1}{\epsilon^2} - \frac{31}{30\epsilon} \right] \quad (\text{B.13})$$

$$I_{3c} = -\frac{1}{\epsilon^2} \frac{(1+\beta^2)}{2\beta} \ln[(1-\beta)/(1+\beta)] \quad (\text{B.14})$$

In terms of the cusp angle

$$\gamma = \ln \left(\frac{v_i \cdot v_j + \sqrt{(v_i \cdot v_j)^2 - v_i^2 v_j^2}}{\sqrt{v_i^2 v_j^2}} \right) \quad (\text{B.15})$$

and

$$\coth \gamma = \frac{v_i \cdot v_j}{\sqrt{(v_i \cdot v_j)^2 - v_i^2 v_j^2}} \quad (\text{B.16})$$

the previous results for the integrals can be written as

$$I_{1a} = -\frac{1}{\epsilon} \gamma \coth \gamma \quad (\text{B.17})$$

$$I_{2a} + I_{2b} = -\frac{1}{2\epsilon^2}\gamma^2 \coth^2 \gamma \quad (\text{B.18})$$

$$I_{2b} = \frac{1}{2\epsilon} \coth^2 \gamma \left\{ \gamma \left[\text{Li}_2(e^{-2\gamma}) + \zeta_2 \right] + \frac{\gamma^3}{3} + \text{Li}_3(e^{-2\gamma}) - \zeta_3 \right\} \quad (\text{B.19})$$

$$I_{2cq} = \frac{n_f}{3} \gamma \coth \gamma \left[-\frac{1}{\epsilon^2} + \frac{5}{6\epsilon} \right] \quad (\text{B.20})$$

$$I_{2cg} = \left[-\frac{5}{12\epsilon^2} + \frac{31}{72\epsilon} \right] \gamma \coth \gamma \quad (\text{B.21})$$

$$I_{2d} = \frac{1}{2} \coth \gamma \left\{ \frac{1}{\epsilon^2} \gamma + \frac{1}{\epsilon} \left[\frac{\gamma^2}{2} - \gamma + \gamma \ln(1 - e^{-2\gamma}) - \frac{1}{2} \text{Li}_2(e^{-2\gamma}) + \frac{\zeta_2}{2} \right] \right\} \quad (\text{B.22})$$

$$I_{2f} = \frac{1}{\epsilon} \left\{ -\frac{1}{4} [2\zeta_2 + \gamma^2] [-\gamma \coth \gamma + 1] - \frac{1}{6} \gamma^3 \coth \gamma \right\} \quad (\text{B.23})$$

$$I_{3c} = \frac{1}{\epsilon^2} \gamma \coth \gamma \quad (\text{B.24})$$

The above expressions simplify when one of the quarks is massless. In that case $\coth \gamma = 1$ and

$$\gamma = \ln \left(\frac{2v_i \cdot v_j}{\sqrt{v_i^2 v_j^2}} \right) \quad (\text{B.25})$$

The integrals listed before then take simpler forms:

$$I_{1a} = -\frac{1}{\epsilon} \gamma \quad (\text{B.26})$$

$$I_{2a} + I_{2b} = -\frac{1}{2\epsilon^2} \gamma^2 \quad (\text{B.27})$$

$$I_{2b} = \frac{1}{2\epsilon} \left[\frac{\gamma^3}{3} + \zeta_2 \gamma - \zeta_3 \right] \quad (\text{B.28})$$

$$I_{2cq} = \frac{n_f}{3} \gamma \left[-\frac{1}{\epsilon^2} + \frac{5}{6\epsilon} \right] \quad (\text{B.29})$$

$$I_{2cg} = \left[-\frac{5}{12\epsilon^2} + \frac{31}{72\epsilon} \right] \gamma \quad (\text{B.30})$$

$$I_{2d} = \frac{1}{2\epsilon^2} \gamma + \frac{1}{2\epsilon} \left[\frac{\gamma^2}{2} - \gamma + \frac{\zeta_2}{2} \right] \quad (\text{B.31})$$

$$I_{2f} = \frac{1}{\epsilon} \left[\frac{1}{12} \gamma^3 - \frac{1}{4} \gamma^2 + \frac{\zeta_2}{2} \gamma - \frac{\zeta_2}{2} \right] \quad (\text{B.32})$$

$$I_{3c} = \frac{1}{\epsilon^2} \gamma \quad (\text{B.33})$$

References

- [1] W. Wagner, Rept. Prog. Phys. **68**, 2409 (2005) [hep-ph/0507207]; A. Quadt, Eur. Phys. J. C **48**, 835 (2006); R. Kehoe, M. Narain, and A. Kumar, Int. J. Mod. Phys. A **23**, 353 (2008), arXiv:0712.2733 [hep-ex]; T. Han, Int. J. Mod. Phys. A **23**, 4107 (2008), arXiv:0804.3178 [hep-ph]; W. Bernreuther, J. Phys. G **35**, 083001 (2008), arXiv:0805.1333 [hep-ph]; D. Wackerth, 0810.4176 [hep-ph]; M.-A. Pleier, Int. J. Mod. Phys. A **24**, 2899 (2009), 0810.5226 [hep-ex]; J.R. Incandela, A. Quadt, W. Wagner, and D. Wicke, Prog. Part. Nucl. Phys. **63**, 239 (2009), 0904.2499 [hep-ex]; W. Wagner, arXiv:1003.4359 [hep-ex].
- [2] D0 Collaboration, V.M. Abazov *et al.*, Phys. Rev. Lett. **103**, 092001 (2009), arXiv:0903.0850 [hep-ex]; Phys. Lett. B **682**, 363 (2010), arXiv:0907.4259 [hep-ex]; arXiv:0912.1066 [hep-ex].
- [3] CDF Collaboration, T. Aaltonen *et al.*, Phys. Rev. Lett. **103**, 092002 (2009), arXiv:0903.0885 [hep-ex]; Phys. Rev. D **81**, 072003 (2010), arXiv:1001.4577 [hep-ex]; arXiv:1004.1181 [hep-ex].
- [4] E. Palencia, arXiv:0905.4279 [hep-ex]; D. Gillberg, arXiv:0906.0523 [hep-ex]; Tevatron Electroweak Working Group, arXiv:0908.2171 [hep-ex]; R. Schwienhorst, arXiv:0908.4553 [hep-ex]; A.P. Heinson, arXiv:0909.4518 [hep-ex]; C.E. Gerber, arXiv:0909.4794 [hep-ex]; L. Li, AIP Conf.Proc.1200, 666 (2010), arXiv:0911.1150 [hep-ex]; A.P. Heinson, Mod. Phys. Lett. A **25**, 309 (2010), arXiv:1002.4167 [hep-ex].
- [5] S.H. Zhu, Phys. Lett. B **524**, 283 (2002) [hep-ph/0109269]; (E) B **537**, 351 (2002).
- [6] S.H. Zhu, Phys. Rev. D **67**, 075006 (2003) [hep-ph/0112109].
- [7] T. Plehn, Phys. Rev. D **67**, 014018 (2003) [hep-ph/0206121].
- [8] E.L. Berger, T. Han, J. Jiang, and T. Plehn, Phys. Rev. D **71**, 115012 (2005) [hep-ph/0312286].
- [9] N. Kidonakis and G. Sterman, Phys. Lett. B **387**, 867 (1996); Nucl. Phys. B **505**, 321 (1997) [hep-ph/9705234]; N. Kidonakis, G. Oderda, and G. Sterman, Nucl. Phys. B **531**, 365 (1998) [hep-ph/9803241].
- [10] N. Kidonakis, Phys. Rev. D **74**, 114012 (2006) [hep-ph/0609287].
- [11] N. Kidonakis, Phys. Rev. D **75**, 071501(R) (2007) [hep-ph/0701080].
- [12] N. Kidonakis, Acta Phys. Polon. B **39**, 1593 (2008), arXiv:0802.3381 [hep-ph]; Nucl. Phys. A **827**, 448c (2009), arXiv:0901.2155 [hep-ph]; PoS (DIS 2010) 196, arXiv:1005.3330 [hep-ph].
- [13] N. Kidonakis, JHEP **05** (2005) 011 [hep-ph/0412422].

- [14] N. Kidonakis, *Mod. Phys. Lett. A* **19**, 405 (2004) [hep-ph/0401147]; PoS (CHARGED2008) 003 (2008), arXiv:0811.4757 [hep-ph].
- [15] N. Kidonakis, *Phys. Rev. Lett.* **102**, 232003 (2009), arXiv:0903.2561 [hep-ph].
- [16] N. Kidonakis, in *DPF 2009*, arXiv:0910.0473 [hep-ph]; PoS (DIS 2010) 115, arXiv:1005.3849 [hep-ph].
- [17] N. Kidonakis, *Phys. Rev. D* **81**, 054028 (2010), arXiv:1001.5034 [hep-ph].
- [18] G.P. Korchemsky and A.V. Radyushkin, *Phys. Lett. B* **171**, 459 (1986); *Nucl. Phys.* **B283**, 342 (1987); *Phys. Lett. B* **279**, 359 (1992) [hep-ph/9203222].
- [19] J. Kodaira and L. Trentadue, *Phys. Lett.* **112B**, 66 (1982).
- [20] S.M. Aybat, L.J. Dixon, and G. Sterman, *Phys. Rev. D* **74**, 074004 (2006) [hep-ph/0607309].
- [21] N. Kidonakis, *Phys. Rev. D* **73**, 034001 (2006) [hep-ph/0509079].
- [22] G. Sterman, *Nucl. Phys. B* **281**, 310 (1987).
- [23] S. Catani and L. Trentadue, *Nucl. Phys. B* **327**, 323 (1989).
- [24] H. Contopanagos, E. Laenen, and G. Sterman, *Nucl. Phys. B* **484**, 303 (1997) [hep-ph/9604313].
- [25] N. Kidonakis and R. Vogt, *Phys. Rev. D* **68**, 114014 (2003) [hep-ph/0308222]; *Phys. Rev. D* **78**, 074005 (2008), arXiv:0805.3844 [hep-ph].
- [26] A.D. Martin, W.J. Stirling, R.S. Thorne, and G. Watt, *Eur. Phys. J. C* **63**, 189 (2009), arXiv:0901.0002 [hep-ph].